Physics Letters B 785 (2018) 610–614

Contents lists available at ScienceDirect

Physics Letters B

www.elsevier.com/locate/physletb

Dark matter (DM) searches through studying DM-nucleon coupling strength

D.-M. Mei [a,b,*], W.-Z. Wei [a]

[a] Department of Physics, The University of South Dakota, Vermillion, SD 57069, United States of America
[b] School of Physics and Optoelectronic, Yangtze University, Jingzhou 434023, China

ARTICLE INFO

Article history:
Received 8 May 2018
Received in revised form 1 August 2018
Accepted 31 August 2018
Available online 14 September 2018
Editor: H. Peiris

Keywords:
Dark matter detection
WIMP
Coupling strength

ABSTRACT

Dark matter (DM) interacts with ordinary matter through weakly coupling to nucleons. We analyze the coupling strength for DM-proton and DM-neutron respectively utilizing the available data from the most sensitive experiments, XENON1T and SuperCDMS, for a higher (>10 GeV/c^2) and a lower mass (<10 GeV/c^2) range of DM particles. Subsequently, we calculate the coupling strength constrained by the DAMA claim and a similar experiment (KIMS) using CsI. The results indicate that XENON1T and SuperCDMS are almost fully sensitive to the DM-nucleon coupling strength predicted by the Fermi weak interaction in the higher mass range. As a result, XENON1T is sensitive to the expected small energy associated with the DM-nucleon weak interaction and hence XENON1T provides a strong constrain on the effective mass of DM from $\sim$1 MeV/c^2 to $\sim$100 MeV/c^2, which excludes the mass range of DM between 10 GeV/c^2 to 10^4 GeV/c^2 from being detected. In the lower mass range, four experiments are all not sensitive to the DM-nucleon coupling strength expected from the Fermi weak interaction. The DM-nucleon coupling strength, $(Zf_p + Nf_n)^2$, determined by the DAMA data can be fully ruled out by the most sensitive experiments. This work launches new direction for the current DM experiments to provide the constrains on DM-nucleon coupling strength, which sheds light on DM-nucleon coupling properties between impinging DM particles and target nucleons with null experimental results.

1. Introduction

Dark matter (DM) elastically scattering off ordinary matter via weak interaction is the basis of direct searches for DM with underground experiments [1–21]. These experiments have sensitivity to WIMPs (weakly interacting massive particles) with mass greater than 6 GeV/c^2. The best sensitivity for WIMPs masses above 10 GeV/c^2, with a minimum of 7.7×10^{-47} cm^2 for 35 GeV/c^2, is given by the most recent results from XENON1T [18,22]. Great efforts have been made, WIMPs remain undetected. More experimental results will soon become available through [23,24]. The LZ experiment will push the experimental sensitivity for WIMPs with mass greater than 10 GeV/c^2 very close to the boundary where neutrinos induced backgrounds begin to constrain the experimental sensitivity [25,26].

DM coupling to visible matter is assumed through weak interaction and gravitational interaction [27,28]. A common search channel is elastic scattering between incoming DM particles and target nucleus. Current direct detection experiments search for nuclear recoils caused by DM scattering. The direct detection results based on a differential rate with spin-independent (SI) interactions is given below:

$$\frac{dR}{dE}(E,t) = \frac{\rho_0}{2\mu_{\chi N}^2 \cdot m_\chi} \cdot \sigma_0^{SI} \cdot \varepsilon(E) \cdot F^2(E) \int_{v_{min}}^{v_{esc}} \frac{f(v,t)}{v} dv, \qquad (1)$$

where $\frac{dR}{dE}$ is the differential event rate, dR, with respect to the nuclear recoil energy interval, dE; E is the nuclear recoil energy; t is the time of the measurement; $\rho_0 = 0.4$ GeV/cm^3 (local DM density) [29]; $\mu_{\chi N}$ is the reduced mass of DM-nucleus; m_χ is the mass of DM; σ_0^{SI} is the DM-nucleus cross section at the zero momentum transfer; $\varepsilon(E)$ is the detection efficiency for a given energy transfer between DM and nucleus; $F(E)$ is the nuclear form factor; v is the velocity of DM particles; $v_{esc} = 544$ km/s (the

* Corresponding author at: Department of Physics, The University of South Dakota, Vermillion, SD 57069, United States of America.
E-mail address: Dongming.Mei@usd.edu (D.-M. Mei).

https://doi.org/10.1016/j.physletb.2018.08.074

escape velocity) [30], which is the maximum velocity of WIMPs bound in the potential well of the galaxy; and the minimum velocity is defined as:

$$v_{min} = \sqrt{\frac{m_N E_r}{2\mu_{\chi N}^2}}, \tag{2}$$

with E_r being the detection energy threshold and m_N the mass of nucleus. Finally, the DM velocity profile is commonly described by an isotropic Maxwell–Boltzmann distribution [31]:

$$f(v) = \frac{1}{(2\pi\sigma^2)^{3/2}} exp(-\frac{v^2}{2\sigma^2}), \tag{3}$$

where $\sigma = \sqrt{3/2}v_c$ and $v_c = 220$ km/s describing the average velocity of the Sun around the galaxy. For SI interactions, the cross-section at zero momentum transfer can be expressed as [32]:

$$\sigma_0^{SI} = \sigma_p \cdot \frac{\mu_{\chi N}^2}{\mu_p^2} \cdot [Z \cdot f_p + (A - Z) \cdot f_n]^2, \tag{4}$$

where σ_p is the DM-nucleon cross section; f_p and f_n are the contributions of protons and neutrons to the total coupling strength, respectively; μ_p is the WIMP-nucleon reduced mass; Z represents the number of protons and A is the nuclear mass number. It is common that $f_p = f_n$ is assumed (isospin-conserving) and the dependence of the cross-section with the number of nucleons A takes an A^2 form or A^4 form when $m_\chi \geq m_N$.

The detection efficiency, $\varepsilon(E)$, is usually determined experimentally by calibrating a detector using various radiative sources. The calibration can be normalized to a 100% efficiency for a well-known energy peak, for instance 122 keV from ^{57}Co, of electronic recoils. This assumes that the electronic recoils from 122 keV γ ray can be fully observed in a given detector. Therefore, the detection efficiency is also called a relative detection efficiency. The relative detection efficiency of nuclear recoils is then determined by taking into account the ionization efficiency and quenching effect [33]. The relative detection efficiency of low-energy electronic recoils can also be determined through normalization. The discrimination efficiency between nuclear recoils and electronic recoils, as part of the relative detection efficiency, is often determined through calibration and modeling [34–37].

A commonly used nuclear form factor, F, can be expressed in the exponential form as below [38,39]:

$$F(E) = exp(-E/2Q_0), \tag{5}$$

where E is the energy transfered from the DM to the nucleus, $Q_0 = 1.5\hbar^2/(m_N R_0^2)$ is the nuclear coherence energy and $R_0 = 10^{-13}$ cm $[0.3 + 0.91(m_N/\text{GeV})^{1/3}]$ is the radius of the nucleus. Note that $\hbar$ is the reduced Planck constant.

Using eqs. (1)–(5), the current experiments interpret their experimental results by extracting the parameter space of DM-nucleon cross section versus the mass of DM particles when the measurements are constrained by the background events in the region of interest (ROI). As an example, we show the expected DM-nucleon cross section versus the mass of DM particles from the most recent XENON1T [18] (Fig. 1) by incorporating their mass exposure, detection efficiency and the background events in the ROI.

It is important to point out that the plotted DM-nucleon cross section (versus the mass of DM particles) in Fig. 1 is the product of $\sigma_p f_{n,p}^2$ assuming $f_p = f_n$. However, f_p is not necessarily equal to f_n for weak interaction. In fact, isospin can be violated in weak interaction [40–48] between an incoming DM particle and a nucleus.

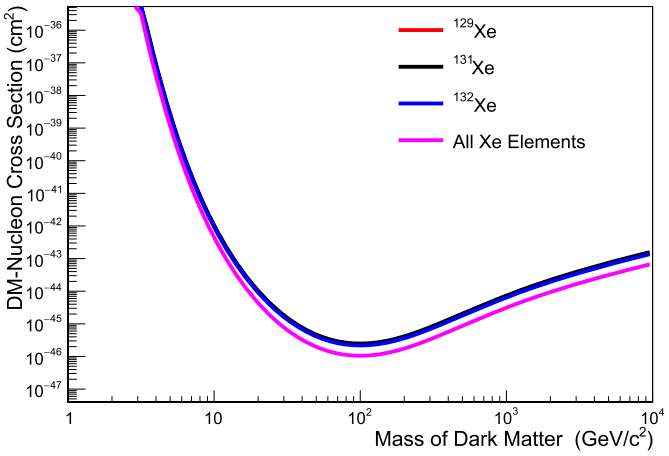

Fig. 1. The expected DM-nucleon cross section versus the mass of DM particles from XENON1T [18]. Note that the most abundant elements ^{129}Xe, ^{131}Xe, and ^{132}Xe are used in the calculation. For the sake of simplicity, the reported background events are treated uniformly across the entire ROI. (For interpretation of the colors in the figure(s), the reader is referred to the web version of this article.)

If one sticks to eq. (4) by considering a more general form of relation between coupling coefficients, f_p and f_n, the experimental results can then be used to constrain the values of f_p and f_n with respect to the mass of DM particles if σ_p is known.

2. Cross section

In eq. (4), σ_p represents a cross section of nucleon subtended to the impinging DM particles. A cross section can be well defined as a measure of the effective surface area of a nucleon seen by the impinging DM particles. For the weak interaction between the impinging DM particles and a nucleon, the effective surface area seen by the impinging DM particles can be expressed to be $\sigma_p = \pi \cdot (\hbar/M_Z c)^2$, assuming that Z boson is the weak force mediator between a DM particle and a nucleon with M_Z being the mass of Z boson and c the speed of light in vacuum. Note that the term $(\hbar/M_Z c = 2.17 \times 10^{-18}$ m) represents the effective range of weak force. Beyond this range, the weak force between the impinging DM particles and a nucleon is extremely small and no effective weak interaction can occur. On the other hand, if DM particles enter this range, the observable quantity – the nuclear recoil energy, is solely dependent upon the weak interaction coupling coefficients, f_p and f_n, and their relationship. Since the coupling coefficients, f_p and f_n, can be different from each other, the experiments with sensitivity to f_p and f_n can be used to constrain the values of f_p and f_n. This launches new direction for the current DM experiments to provide their constrains on f_p and f_n, which allows to derive a deeper understanding of DM-nucleon coupling between impinging DM particles and target nucleons.

This effective range can also be derived by utilizing the energy associated with the weak interaction that can be represented as below:

$$E_w = \frac{g_F^2}{4\pi r} exp(-\frac{M_W c r}{\hbar}), \tag{6}$$

where g_F is the effective charge of weak interaction, M_W is the mass of the carrier particles for weak interaction (W and Z bosons). The square of the effective charge of weak interaction for a proton and a DM particle can be expressed as:

$$g_F^2 = \frac{4\pi G_F m_p m_\chi^* c^2}{\hbar^2}, \tag{7}$$

where $G_F = 1.436 \times 10^{-62}$ J m^3 is the Fermi constant and m_p is the mass of proton and m^*_χ is the effective mass of DM participles that responds to the weak force when interacting with nucleons. This is because the movement of DM particles in a periodic weak potential, over long distances larger than the size of nucleons, can be very different from their motion in a vacuum. In the momentum space, $m^*_\chi = \hbar^2 / \frac{d^2E(k)}{dk^2}$, where $E(k)$ is the energy of an incoming DM particle at a wave-vector k. m^*_χ can be measured experimentally if DM particles are found. A null experimental result can be used to constrain the values of m^*_χ.

From eq. (6), we can obtain the effective range of weak interaction in the limit of $r \ll 1/M_W$ for a given nucleon (proton or neutron) as below:

$$r = \frac{g_F^2}{4\pi E_W + g_F^2 M_W c/\hbar}. \tag{8}$$

Subsequently, the cross section σ_p can be expressed as:

$$\sigma_p = \pi \left(\frac{g_F^2}{4\pi E_W + g_F^2 M_W c/\hbar}\right)^2. \tag{9}$$

One can assume that the maximum energy associated with the weak interaction is $E_W = \frac{1}{2} m_\chi v^2$ and $m^*_\chi = m_\chi$. DM-nucleon cross section as a function of the mass of DM given by eq. (9) is a constant (1.48×10^{-31} cm^2), since the energy scale associated with the weak interaction is expected to be in the range of ~10 keV if the mass of DM particles are in the range of ~100 GeV/c^2.

3. Weak coupling strength

As can be seen in eq. (4), once σ_p is determined, the experimental results can be used to constrain the coupling coefficients f_p and f_n. From eq. (1) to (4), the integrated event rate R can be expressed as below:

$$R = \frac{6 \times 10^{26}}{A} \times \frac{2\rho_0 \sigma_p \mu^2_{\chi,N} [Z f_p + (A - Z) f_n]^2}{c^2 \sqrt{\pi} m_\chi \mu_p^2} \int_{E_{th}}^{E} \varepsilon(E) F^2(E) < v > dE \quad \text{s}^{-1}\,\text{kg}^{-1}. \tag{10}$$

Where $< v >= \int_{v_{min}}^{v_{esc}} v f(v) dv$. Rearranging the terms in eq. (10) and using ($A - Z = N$, which stands for the number of neutrons), we have:

$$(Z f_p + N f_n)^2 = \frac{A c^2 \sqrt{\pi} m_\chi \mu_p^2 R}{12 \times 10^{26} \rho_0 \sigma_p \mu^2_{\chi,N} \int_{E_{th}}^{E} \varepsilon(E) F^2(E) < v > dE} \tag{11}$$

One can define $(Z f_p + N f_n)^2 = \alpha_w \alpha_{sw}$, since the term $(Z f_p + N f_n)^2$ represents the DM-nucleon coupling strength. The term, α_w, is the intrinsic weak coupling constant under the Fermi theory [49] and α_{sw} stands for the super weak coupling strength contributed by protons and neutrons. The intrinsic weak coupling strength can be calculated using $\alpha_w = 8 G_F m_Z^2 / 4\pi\sqrt{2}(\hbar c)^3$ stated in the standard (Fermi) weak interaction [50]. The super weak coupling strength is also called "running coupling constant", which is energy dependent. Using eq. (6), we define α_{sw} to be: $\alpha_{sw} = E_w / E_{ph}$, where $E_{ph} = \hbar c / r$ and r is given by eq. (8). Therefore, α_{sw} is a relative weak coupling strength.

For an experiment with a null result in the ROI, R is given by the observed background events that constrain the experimental sensitivity. Utilizing the same Z and different N from an experiment such as XENON1T and SuperCDMS [51], one can compute f_p and f_n respectively with eq. (11). For DAMA [52] and KIMS [53], we employ ^{23}Na, ^{127}I, and ^{133}Cs for the calculations of f_p and f_n. Figs. 2 and 3 show the coupling coefficients versus the mass of DM particles.

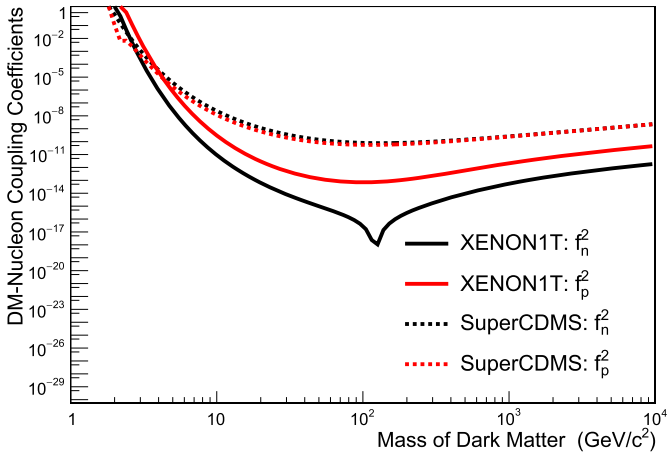

Fig. 2. Shown is the effective coupling coefficients versus the mass of DM particles constrained by the XENON1T data with a mass exposure of 1040 kg for 34.2 days and the SuperCDMS data with a mass exposure of 612 kg days. The most abundant elements ^{129}Xe, ^{131}Xe, ^{132}Xe, ^{70}Ge, ^{72}Ge, and ^{74}Ge are employed in obtaining DM-nucleon coupling coefficients, f_p^2 and f_n^2.

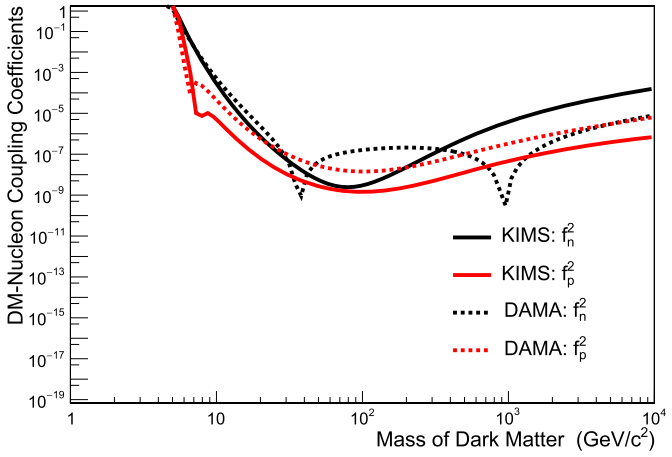

Fig. 3. Shown is the effective coupling coefficients versus the mass of DM particles constrained by the KIMS data with a mass exposure of 24524.3 kg days and the DAMA claim.

One can use the effective atomic number and the average atomic mass to obtain the coupling strength for NaI and CsI. The effective atomic number can be calculated as [54]: $Z_{eff} = \sqrt[2.94]{f_1 \cdot Z_1^{2.94} + f_2 \cdot Z_2^{2.94}}$, where $f_1 = \frac{Z_1}{Z_1+Z_2}$, $f_2 = \frac{Z_2}{Z_1+Z_2}$, Z_1 and Z_2 are atomic number of elements in NaI and CsI, respectively. Fig. 4 displays the DM-nucleon coupling for Xe, Ge, NaI, and CsI.

4. Results and discussion

It is noticed from Figs. 2 and 3 that: (1) XENON1T is more sensitive to f_n^2 while SuperCDMS and KIMS are more sensitive to f_p^2; (2) DAMA is sensitive to f_p^2 or f_n^2, depending on the mass range of DM particles; (3) in the lower mass range (<10 GeV/c^2), f_p^2 and f_n^2 start to merge together; (4) the curves of f_p^2 and f_n^2 constrained by the DAMA claim can be fully excluded in the lower mass range by

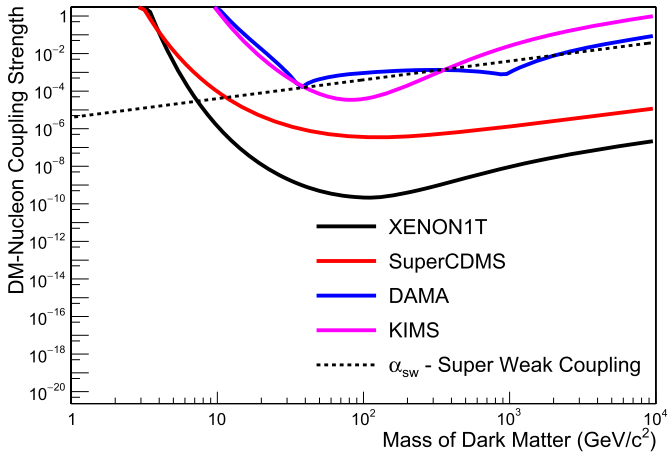

Fig. 4. Shown is the effective coupling strength, $\alpha_{sw} = (Z \times f_p + N \times f_n)^2/\alpha_w$, versus the mass of DM particles.

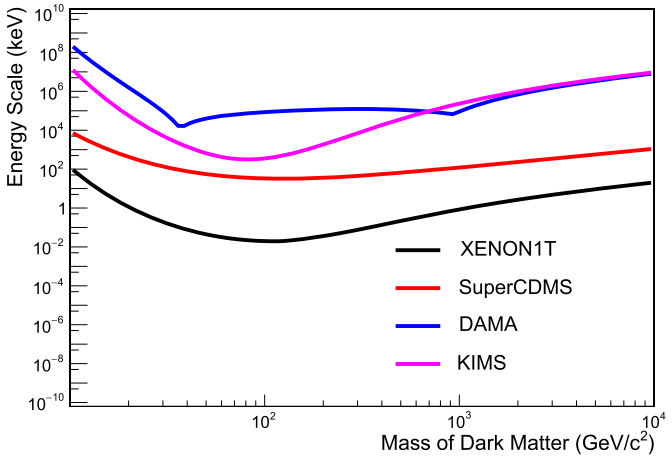

Fig. 5. Shown is the constrained energy scale versus the mass of DM particles determined by the experimental data.

SuperCDMS with a sensitivity of greater than 6 GeV/c^2 and in the higher mass range by XENON1T with a sensitivity of greater than 10 GeV/c^2; and (5) KIMS can partially exclude the DAMA claim.

Fig. 4 shows the super weak coupling strength, $\alpha_{sw} = (Zf_p + Nf_n)^2/\alpha_w$, constrained by the experimental data from XENON1T, SuperCDMS, DAMA, and KIMS together with the predicted α_{sw} as a function of the mass of DM particles assuming $m^*_\chi = m_\chi$. It is clear that DAMA and KIMS are only partially sensitive to the weak coupling strength predicted by the Fermi theory. This suggests that the DAMA claim may not be due to the weak interaction of DM-nucleon coupling under the standard Fermi coupling. SuperCDMS has sensitivity to the predicted α_{sw} for the mass range from 15 GeV/c^2 to 10^4 GeV/c^2. Only XENON1T excludes the predicted values of α_{sw} from 10 GeV/c^2 to 10^4 GeV/c^2. Note that the values of α_{sw} in the higher mass range (>10 GeV/c^2) constrained by the XENON1T data is much smaller than the predicted standard Fermi weak coupling strength. This implies that the energy associated with the DM-nucleon weak coupling is really small.

Utilizing the values of α_{sw} constrained by the experimental data (see Fig. 4), one can obtain the constrained energy ($E_w = \alpha_{sw} E_{ph}$) associated with the weak interaction, as shown in Fig. 5. As can be seen that only XENON1T is sensitive to the expected small energy in the range of ∼10 keV associated with DM-nucleon weak interaction. Since the constrained energy, E_w, is connected to the effective mass of DM particles through eq. (6) and (7), one can

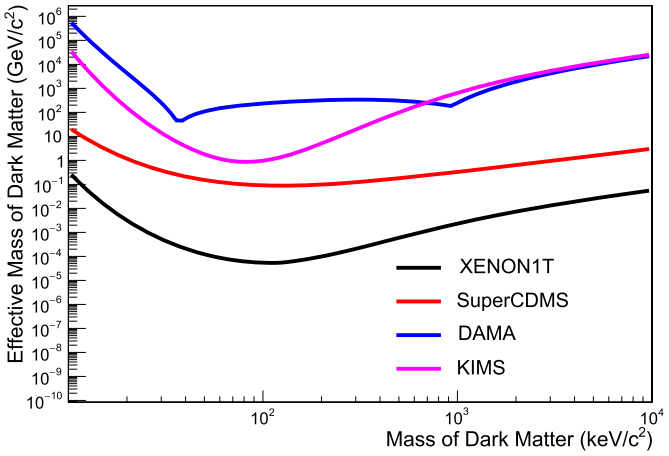

Fig. 6. Shown is the constrained effective mass of DM particles versus the mass of DM particles determined by using the experimental data.

determine the constrained effective mass of DM particles for different targets, as shown in Fig. 6. It is shown that DAMA and KIMS are sensitive to the effective mass of DM greater than 10 GeV/c^2. SuperCDMS has a sensitivity to the effective mass of DM down to 1 GeV/c^2. XENON1T provides a much stronger constrain on the effective mass of DM from ∼1 MeV/c^2 to ∼100 MeV/c^2, which excludes the mass range of DM between 10 GeV/c^2 to 10^4 GeV/c^2 from being detected. This is because the effective mass range of ∼1 MeV/c^2 to ∼ 100 MeV/c^2 corresponds to the constrained energy available for weak interaction from ∼100 keV to below 1 keV. Hence, the resulted nuclear recoil energy would fall below the detection threshold of XENON1T, since XENON1T has announced a null result.

In summary, this work provides a new framework to analyze the experimental data in the searches for DM. The result of a super weak coupling strength implies that the effective mass of DM is small, which results in a very small energy associated with DM-nucleon coupling. XENON1T has largely excluded the effective mass of DM particles. This suggests to search for DM for the mass below 10 GeV/c^2 or even lower down to MeV/c^2 where the large parameters space is unexplored [55,56].

Acknowledgements

This work is supported in part by NSF OIA 1743790, DOE grant DE-FG02-10ER46709, DOE grant DE-SC0004768, the Office of Research at the University of South Dakota and a research center supported by the State of South Dakota.

References

[1] CDMS Collaboration, Z. Ahmed, et al., Phys. Rev. Lett. 102 (2009) 011301, arXiv:0802.3530.
[2] CDEX and TEXONO Collaboration, S. Liu, et al., Phys. Rev. D 90 (3) (2014) 032003, arXiv:1403.5421.
[3] CoGeNT Collaboration, C. Aalseth, et al., Phys. Rev. Lett. 101 (2008) 251301, arXiv:0807.0879.
[4] CRESST Collaboration, G. Angloher, et al., Eur. Phys. J. C 72 (2012) 1971, arXiv:1109.0702.
[5] COUPP Collaboration, E. Behnke, et al., Phys. Rev. D 86 (2012) 052001, arXiv:1204.3094.
[6] DAMIC Collaboration, J. Barreto, et al., Phys. Lett. B 711 (2012) 264, arXiv:1105.5191.
[7] DAMA/LIBRA Collaboration, R. Bernabei, et al., Eur. Phys. J. C 67 (2010) 39, arXiv:1002.1028.
[8] DarkSide Collaboration, M. Bossa, et al., J. Instrum. 9 (2014) C01034.
[9] DRIFT Collaboration, J.B.R. Battat, et al., Phys. Dark Universe 9 (2014) 1, arXiv:1410.7821.

[10] EDELWEISS Collaboration, E. Armengaud, et al., Astropart. Phys. 47 (2013) 1, arXiv:1305.3628.
[11] KIMS Collaboration, S.-C. Kim, J. Phys. Conf. Ser. 384 (2012) 012020.
[12] LUX Collaboration, D.S. Akerib, et al., Phys. Rev. Lett. 118 (2) (2017) 021303, arXiv:1608.07648.
[13] PandaX Collaboration, M. Xiao, et al., Sci. China, Phys. Mech. Astron. 57 (2014) 2024, arXiv:1408.5114.
[14] PICO Collaboration, C. Amole, et al., Phys. Rev. Lett. 114 (23) (2015) 231302, arXiv:1503.00008.
[15] SuperCDMS Collaboration, R. Agnese, et al., Phys. Rev. Lett. 112 (2014) 241302, arXiv:1402.7137.
[16] XENON Collaboration, E. Aprile, et al., Astropart. Phys. 34 (2011) 679, arXiv:1001.2834.
[17] XENON100 Collaboration, E. Aprile, et al., Science 349 (2015) 851, arXiv:1507.07747.
[18] XENON Collaboration, E. Aprile, et al., Phys. Rev. Lett. 119 (2017) 181301, arXiv:1705.06655v1.
[19] XMASS Collaboration, K. Abe, et al., Astropart. Phys. 31 (2009) 290, arXiv:0809.4413.
[20] ZEPLIN-III Collaboration, D.Y. Akimov, et al., Phys. Lett. B 692 (2010) 180, arXiv:1003.5626.
[21] DEAP Collaboration, M. Boulay, J. Phys. Conf. Ser. 375 (2012) 012027, arXiv:1203.0604.
[22] XENON Collaboration, E. Aprile, et al., arXiv:1805.12562.
[23] MINICLEAN Collaboration, K. Rielage, et al., Phys. Proc. 61 (2015) 144, arXiv:1403.4842.
[24] LZ Collaboration, D.S. Akerib, et al., arXiv:1509.02910.
[25] L.E. Strigari, New J. Phys. 11 (2009) 105011, arXiv:0903.3630.
[26] A. Gutlein, et al., Astropart. Phys. 34 (2010) 90, arXiv:1003.5530.
[27] G. Jungman, M. Kamionkowski, K. Griest, Phys. Rep. 267 (1996) 195–373.
[28] P.F. Smith, J.D. Lewin, Phys. Rep. 187 (1990) 203–280.
[29] Brian Feldstein, Felix Kahlhoefer, J. Cosmol. Astropart. Phys. 1408 (2014) 065.
[30] M.C. Smith, et al., Mon. Not. R. Astron. Soc. 379 (2007) 755.
[31] Mariangela Lisanti, arXiv:1603.03797.
[32] Teresa Marrodán Undagoitia, Ludwig Rauch, J. Phys. G 43 (1) (2016) 013001.
[33] J. Lindhard, et al., Range concepts and heavy ion ranges (notes on atomic collisions, II), Mat.-Fys. Medd. Danske Vid. Selsk. 33 (14) (1963) 1.
[34] D. Barker, D.-M. Mei, Astropart. Phys. 38 (2012) 1–6.
[35] D. Barker, et al., Astropart. Phys. 48 (2013) 8–15.
[36] L. Wang, D.-M. Mei, Journal of Physics G: Nuclear and Particle Physics 44 (2017) 055001.
[37] Szydagis, et al., J. Instrum. 6 (2011) P10002.
[38] S.P. Ahlen, et al., Phys. Lett. B 264 (1991) 114.
[39] K. Freese, J. Frieman, A. Gould, Phys. Rev. D 37 (1988) 3388.
[40] Jonathan L. Feng, et al., Phys. Lett. B 703 (2011) 124–127.
[41] Jason Kumar, David Sanford, Louis E. Strigari, arXiv:1112.4849.
[42] Yu-Feng Zhou, Nucl. Phys. B, Proc. Suppl. 246-247 (2014) 99–105, arXiv:1212.2043.
[43] R. Martinez, F. Ochoa, arXiv:1512.04128.
[44] Carlos E. Yaguna, arXiv:1610.08683.
[45] Andriy Kurylov, Marc Kamionkowski, Phys. Rev. D 69 (2004) 063503.
[46] James B. Dent, et al., Phys. Rev. D 95 (2017) 051701(R).
[47] Carlos E. Yaguna, Phys. Rev. D 95 (2017) 055015.
[48] F. Giuliani, Phys. Rev. Lett. 95 (2005) 101301.
[49] F.L. Wilson, Am. J. Phys. 36 (12) (1968) 1150.
[50] David Griffiths, Introduction to Elementary Particles, Wiley, 1987, 2nd edn. 2008, Chapter 1.
[51] R. Agnese, et al., SuperCDMS Collaboration, Phys. Rev. D 92 (2015) 072003.
[52] R. Bernabei, et al., Eur. Phys. J. C 56 (2008) 333–355.
[53] H.S. Lee, et al., Phys. Rev. D 90 (2014) 052006.
[54] R.C. Murty, Nature 207 (24 July 1965) 398–399.
[55] R. Essig, J. Mardon, T. Volansky, Phys. Rev. D 85 (2012) 076007.
[56] D.-M. Mei, et al., Eur. Phys. J. C 78 (2018) 187.